


RESEARCH PAPER



Spontaneous formation of tumorigenic hybrids between human omental adipose-derived stromal cells and endometrial cancer cells increased motility and heterogeneity of cancer cells

Mingxia Li^{a,b*}, Xiaoping Li^{a*}, Lijun Zhao^a, Jingyi Zhou^a, Yuan Cheng^a, Bo Xu^c, Jianliu Wang^a, and Lihui Wei ^a

^aDepartment of Gynecology and Obstetrics, Peking University People's Hospital, Beijing, China; ^bDepartment of Gynecology and Obstetrics, People's Liberation Army (PLA) Medical School, Chinese PLA General Hospital, Beijing, China; ^cState Key Laboratory of Natural and Biomimetic Drugs, School of Pharmaceutical Sciences, Peking University, Beijing, China

ABSTRACT

Recent reports indicate that mesenchymal stem cells (MSCs) can fuse with cancer cells to promote cancer progression. Omental adipose-derived stromal cells (O-ASCs) are similar to MSCs, which could be recruited to the stroma in endometrial cancer. The aim of our study was to investigate whether O-ASCs can fuse with endometrial cancer cells to influence cancer cells biological characteristics. We isolated O-ASCs from patients with endometrial cancer. O-ASCs and endometrial cancer cells were labeled with different fluorescent tags and directly co-cultured in an Opera high-throughput spinning-disk confocal microscopy system to observe the processes involved in the fusion, division and migration of hybrid cells. Immunofluorescence and high-throughput imaging analyzes were performed to evaluate proteins related to epithelial-mesenchymal transition (EMT). We found O-ASCs could spontaneously fuse with endometrial cancer cells, including cytomembrane and nuclear fusion. After fusion, endometrial cancer cells assume an elongated and fibroblast-like appearance that exhibit mesenchymal phenotypes. The hybrid cells proliferated through bipolar and multipolar divisions and exhibited more rapid migratory speeds than were observed in the parental cells ($P < 0.01$), potentially because of their EMT-associated changes, including the down-regulation of E-cadherin and up-regulation of Vimentin. Our results collectively suggest that tumorigenic hybrids spontaneously formed between human O-ASCs and endometrial cancer cells, and that the resulting cells enhanced cancer mobility and heterogeneity by accelerated migration and undergoing multipolar divisions. These data provide a new avenue for investigating the roles of O-ASCs in endometrial cancer.

ARTICLE HISTORY

Received 11 May 2018
Revised 7 December 2018
Accepted 12 December 2018

KEYWORDS

Cell fusion; adipose-derived stromal cells; endometrial cancer; EMT; cancer progression

Introduction

Endometrial cancer (EC) is a common gynecologic malignancy that is becoming increasingly prevalent in China and is strongly linked with obesity [1,2]. Excess intra-abdominal adipose tissue further increases the risk and, in some cases, the mortality of intra-abdominal cancers, such as prostate, colon, pancreatic, and endometrial cancer [3–5]. Moreover, abdominal adipose tissue has been associated with colon, breast and endometrial cancers. [6–11]

Recent studies have shown that adipose tissue contains a population of mesenchymal progenitor cells that can facilitate tumor progression [12–15]. Zhang Y et al. found that an increase in white adipose tissue enhanced the recruitment of adipose stem cells (ASCs) to tumor cells, thereby promoting

tumor growth [16]. Prizment et al. reported that ASCs stimulated the migration of breast cancer cells and markedly increased their metastasis to mouse organs [17]. ASCs derived from the abdominal adipose tissues of obese patients promoted breast cancer cell proliferation in vitro [18]. The omentum is a substantially vascularized and innervated fatty tissue that lies over the bowels and is the most common place from which the intraperitoneal dissemination of ovarian cancer and endometrial cancer occurs [19,20]. ASCs derived from the human omentum may promote ovarian cancer proliferation, migration, chemoresistance and radiation resistance in vitro [19]. O-ASCs can also be recruited to tumors, whereupon they enhance endometrial cancer vascularization, thereby promoting the survival and proliferation of tumor cells [20]. In addition,

CONTACT Lihui Wei  weilh@bjmu.edu.cn

*These authors contributed equally to this work.

© 2019 Informa UK Limited, trading as Taylor & Francis Group

specific factors secreted by O-ASCs were dominant contributors to tumor progression [20]. However, whether a direct interaction between O-ASCs and endometrial cancer cells plays a role in these processes remains unclear.

Cell fusion is believed to be a relatively rare and strictly regulated phenomenon in which two or more cells merge their plasma membranes, becoming one cell. This occurs only during specific occasions, such as fertilization, tissue regeneration and cancer [21,22]. The results of an increasing number of studies have suggested that cell fusion may be involved in tumor progression [23–27]. The hybrids that result from cell fusion can be more malignant than their parental cells and possess an enhanced ability to metastasize [28–30]. A “wolf in sheep’s clothing” model has been proposed to explain the link between cell fusion and metastasis. This model suggests that tumor cells become metastatic when they fuse with normal cells traveling freely throughout the body [21]. For instance, fusion between tumor cells and macrophages has been shown to produce hybrid cells with increased metastatic abilities [31]. Tumorigenic hybrids between mesenchymal stem cells and gastric cancer cells enhanced cancer proliferation and migration [32]. The hybrids that formed between lung cancer and bone marrow-derived mesenchymal stem cells enhanced malignancy by epithelial to mesenchymal transition (EMT) and the acquisition of stem cell-like properties [33]. Thus, inducing fusion between tumor cells and bone marrow-derived cells may be an efficient way to promote the rapid acquisition of metastatic phenotypes [34].

ASCs share many features with bone marrow-derived mesenchymal stromal cells (BM-MSC), including cell surface marker expression, plastic adherence, and the capacity to differentiate into cells with a mesenchymal lineage [35,36]. However, few studies have been performed to explore the effect of cell fusion between ASCs and cancer cells on cancer progression. Based on a previous report that showed that O-ASCs could be recruited to the stroma of endometrial cancer, we directly cocultured O-ASCs and endometrial cancer (EC) cells. We were amazed to discover that these two cell lines can spontaneously fuse. Next, we investigated the effects of fusion with O-ASCs on the biological properties of endometrial cancer cells and

found that the hybrids formed by fusion between O-ASCs and endometrial cancer cells contributed to high motility and heterogeneity, as reflected by EMT and multipolar division.

Results

Characterization of O-ASCs

O-ASCs were isolated from three patients with endometrioid EC at FIGO Stages Ia-Ib. As shown in supplemental Figure S1A, all O-ASCs displayed a relatively heterogeneous morphology consisting of both elongated and polygonal cells that exhibited good proliferative ability (Supplemental Figure S1A, S1D). Differentiation assays demonstrated that the O-ASCs were able to differentiate into adipogenic, chondrogenic, and osteogenic mesenchymal lineages (Supplemental Figure S1C). Cell surface markers were also characterized by flow cytometry (Supplemental Figure S1B). The O-ASCs expressed CD29, CD44, CD73, CD90, and CD105, all of which are characteristically found on MSCs [35,36]. In addition, the O-ASCs were negative for the monocyte marker CD11b and the hematopoietic stem cell makers HLA-DR, CD34 and CD45.

Fusion of EC cells with O-ASCs generates hybrid cells

To facilitate the identification of cell fusion events, fusion partners were fluorescently labeled (Green for EC cells and Red for O-ASCs) via transfection by control lentiviral vectors (See Supplemental Figure S2). After the cells were cultured for 48 h *in vitro*, the dynamic process by which the hybrids (double-stained cells) formed was observed and captured by an Opera high-throughput spinning-disk confocal microscopy system. First, we observed that the two kinds of cells migrated and then adhered to each other. Then, a sharp fusion process was observed that consisted of membrane merging and cytoplasmic mixing (see Figure 1). We have compiled the images that were captured at each time point into a video, and this allowed us to clearly observe this dynamic process, as shown in Supplemental Video 1 and 2 (The target cells were labeled in the circle). The hybrid cells had large volumes, like O-ASCs, and contained more than

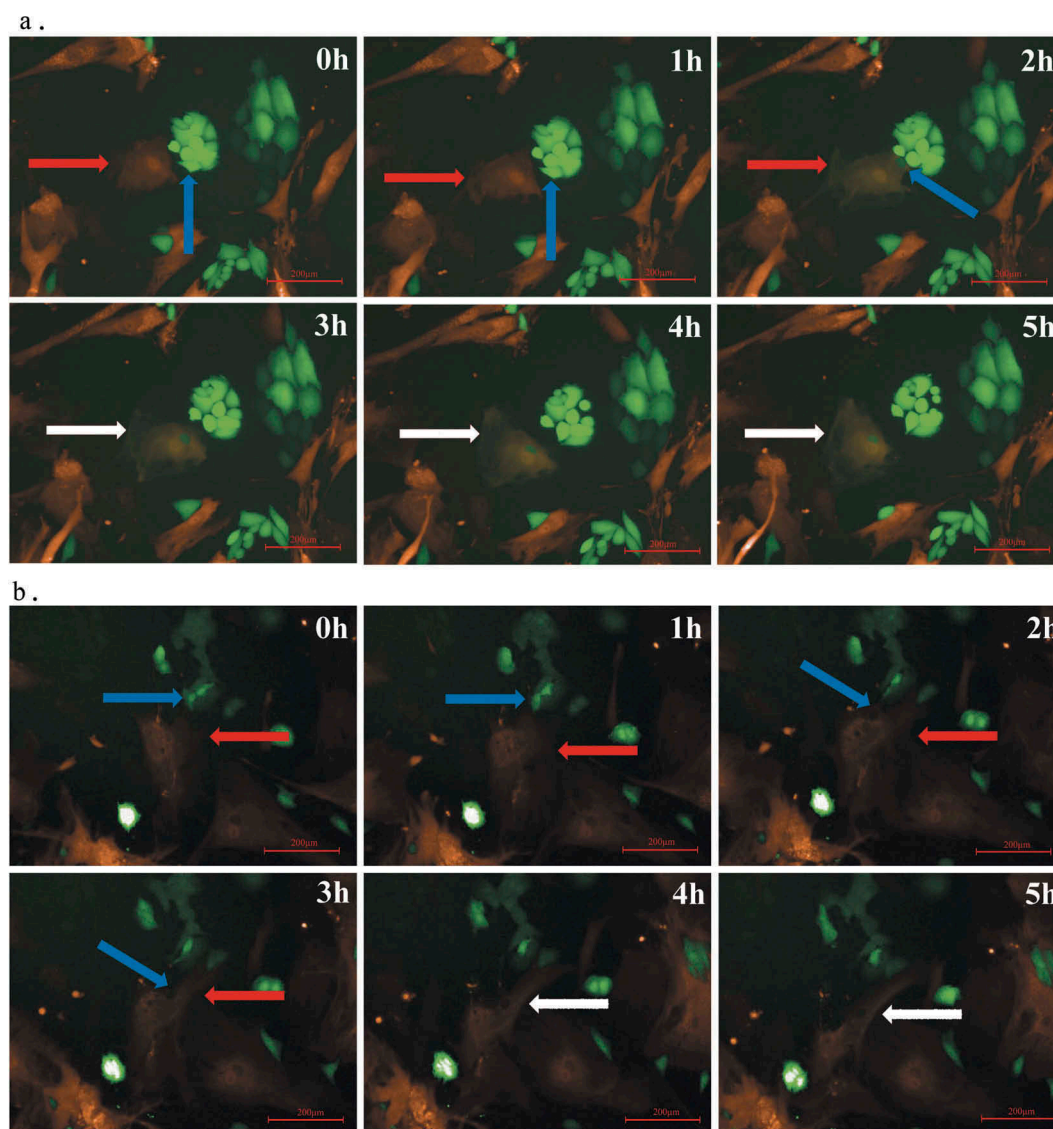


Figure 1. Fusion of O-ASCs and endometrial cancer cells. (a). O-ASCs/RFP (indicated by a red arrow) and Hec-1A/GFP (indicated by a blue arrow) cells were directly co-cultured under a Perkin Elmer Opera High-Content Microscopy System that automatically took fluorescence photographs every 1 h for a continuous 24 h (80X). At the 3 h time point, we observed that fused cells had formed (indicated by white arrow). These cells were double-labelled and did not undergo nuclear fusion. (b). O-ASCs/RFP (indicated by a red arrow) and Ishikawa/GFP (indicated by a blue arrow) cells were directly co-cultured under a Perkin Elmer Opera High Content Microscopy System. At the 4 h time point, fused, double-labelled cells had formed (indicated by a white arrow) but had not undergone nuclear fusion.

two nuclei, potentially for a long period of time, before they suddenly fused together to form a single new, looser and larger nucleus while undergoing cell division (see Figure 3(a)). This dynamic process is clearly shown in Supplemental Video3 and 5.

The fusion efficiencies between RFP-labeled-O-ASCs and GFP-labeled-EC cells were 0.02%-0.4% for Ishikawa cells and 0.06%-0.8% for Hec-1A. When the portion of RFP-labeled-O-ASCs and GFP-labeled-EC cells was 3:1, the fusion efficiency reached the highest.

Hybrid cells were aneuploid and possessed the ability to proliferate

The O-ASCs contained a normal number of chromosomes (45.6 ± 1.1). There were 46.3 ± 1.3 and 58.6 ± 3.0 chromosomes in the Ishikawa EC cells and Hec-1A EC cells, respectively, both of which were close to normal. There were 94.1 ± 8.0 and 114.7 ± 3.3 chromosomes in the fused Ishikawa-ASCs and fused Hec-1A-ASCs cells, respectively. The hybrid cells were therefore aneuploidy (see Figure 2) but not tetraploid.

To study the proliferation of the hybrid cells, the fusion partners were labeled with different fluorescence and directly co-cultured in 96-well plates under an Opera high-throughput spinning-disk confocal microscopy system. We recognized the hybrid cells because they were double-labeled. We observed both normal mitosis and unusual asymmetric divisions and found that the hybrid cells had acquired the ability to proliferate. This process can be divided into the following three stages: (i) the nuclei fused into a single new, looser and larger nucleus 3–4 h before cell division; (ii) these huge hybrid cells abruptly shrank into a much smaller globule; (iii) this small globule exploded into two or three new large and irregular cells (see Figure 3). This continuous and dynamic

process can be observed in the included video (see Supplemental Video 3, 4, and 5).

Cell fusion enhanced migration in EC cells

Morphological observations showed that the parental EC cancer cells mainly displayed rounded and polygonal morphologies. After fusion with O-ASCs, the hybrid cells lost their epithelial morphology, became scattered and exhibited a fibroblast-like appearance with an elongated shape (Figure 1). To further investigate the effect of cell fusion on the ability of cells to migrate, we compared the in vitro migratory speeds of the hybrid cells to the speeds observed in their parental EC cells and O-ASCs. These speeds were captured and calculated using

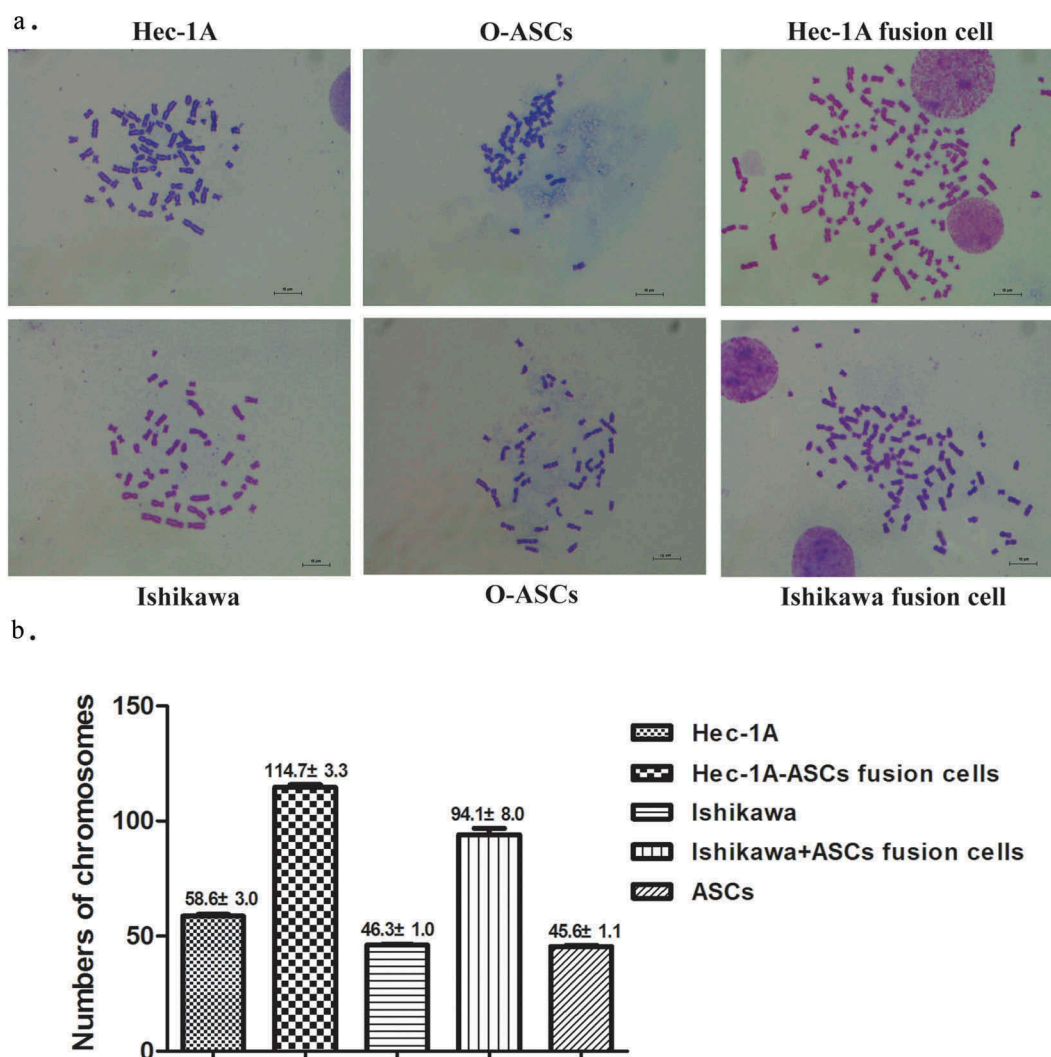


Figure 2. Chromosomes of fused cells and their parental cells. (a). Typical chromosome maps of fused cells and their corresponding parental cells: O-ASCs and Ishikawa or Hec-1A cells (100X). (b). The number of chromosomes in each hybrid and parental cell karyotype.

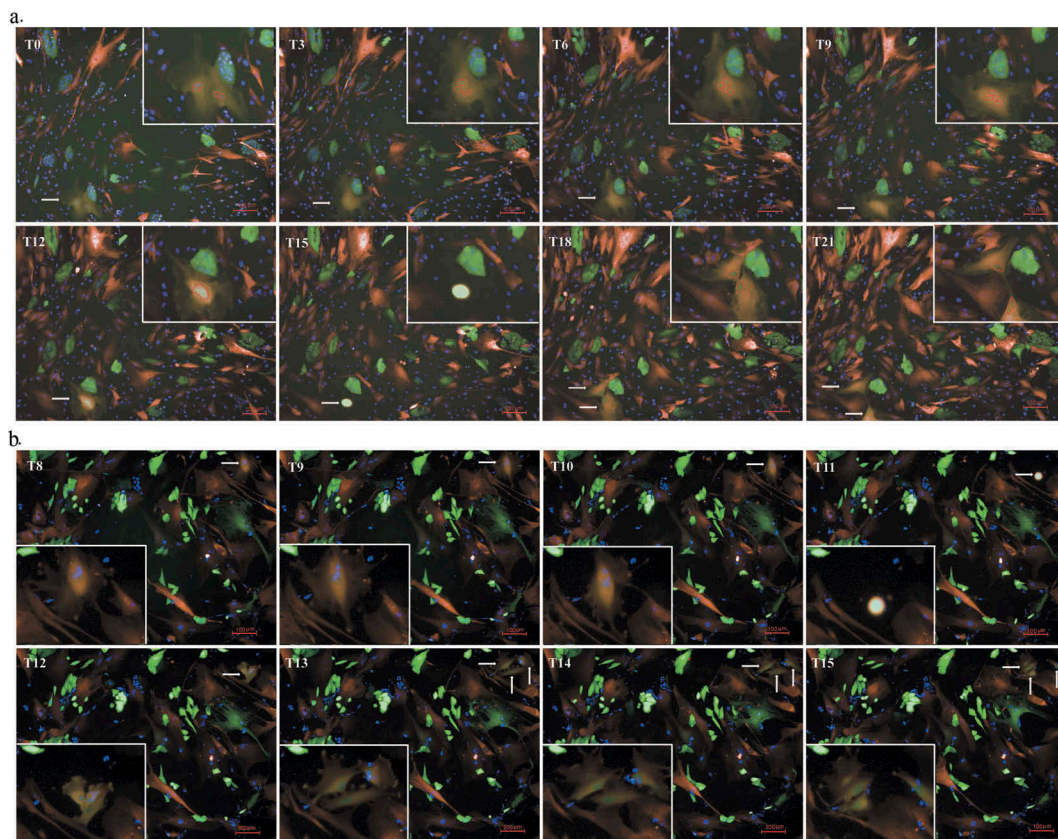


Figure 3. Division of hybrid cells. (a). The process of nuclear fusion and bipolar division in hybrid cells (40X). The fused cell is located in the bottom left corner of the picture. We have shown it at higher power in the top right corner to make it more convenient to observe. From T0 to T9, the fused cell maintained multiple nuclei. At the T12 time point, the nuclei had fused into a large and loose nucleus. In addition, the huge hybrid cells abruptly shrank to form a minimal globule at T15 before exploding into two new, large and irregular cells at T15. (a). The process of multipolar division of hybrid cells (40X). The fused cell is located in the top right corner of the picture. We have shown it at higher power in the bottom left corner so that it is more convenient to observe. This process was similar to that observed during bipolar division before cell division. At T11, the cell also shrank into a bright minimal globule before exploding into three new, large and irregular cells at T12.

an Opera high-throughput spinning-disk confocal microscopy system. We found that the hybrid cells were more active than their parental cells. The migratory speed of the O-ASCs was faster than that observed in the EC cells, but the hybrid cells were even faster (Figure 4). The high migratory speed of the hybrid cells is demonstrated in Supplemental Video 3, 4, and 5. In summary, these data suggest that cell fusion enhances the migratory capacity of EC cells in vitro.

Cell fusion promoted EMT in EC cells

The morphological changes we observed in O-ASC-EC cell hybrids prompted us to hypothesize that the fused cells might undergo EMT. To this end, migratory assays were carried out to determine the migratory capacity of the hybrid cells. In addition, we

found that the hybrid cells' migratory speed was much faster than that observed in their parental cells. To investigate whether EMT-associated genes were differentially expressed between the fused and parental cells, we used immunofluorescence and real-time RT-PCR to determine the expression of EMT related proteins and genes in fused cells and parental cells.

The results of real-time RT-PCR revealed that the level of E-cadherin mRNA in hybrids was obviously down-regulated but the expression of Vimentin in fusion cells were evidently increased (Figure 5(c)). Immunofluorescence also revealed that E-cadherin expression was clearly lower, while vimentin expression was higher in the fused cells than in their parental EC cells (Figure 5(a)). Additionally, a high-throughput imaging analysis revealed that these expression differences were statistically significant

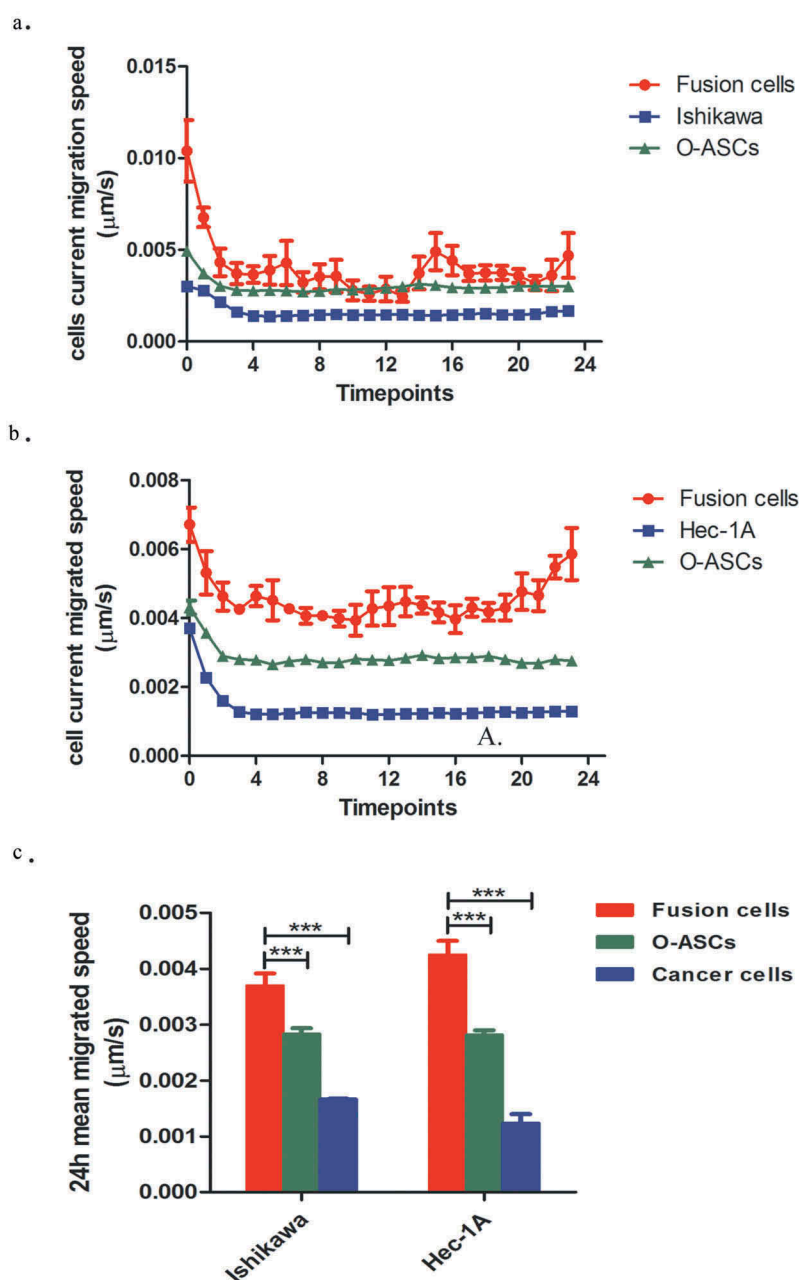


Figure 4. The migratory capabilities of hybrid cells and their parental cells. (a). The horizontal migration speed at each time point was captured and calculated by a Perkin Elmer Opera High Content Microscopy System over a 24 h period. (b). The mean horizontal migratory speeds of the hybrid cells and their parental cells were significantly different ($P < 0.001$). The experiments were repeated three times. The statistical results are presented as Means \pm SD. *** $P < 0.001$.

(Figure 5(b)). In summary, these data suggest that after fusion with O-ASCs, the migratory ability of EC cells was markedly altered, indicating that the hybrid cells underwent EMT.

Discussion

During the processes that occur during tumor progression, tumor cells sometimes exfoliate from

the primary tumor site and spread to other parts of the body. However, the precise mechanisms underlying this process are elusive. The idea that cell fusion contributes to cancer progression was introduced almost 100 years ago when it was proposed that malignancy is a consequence of hybridization between leukocytes and somatic cells [37]. Recently, another prominent theory has emerged that states that a tumor cell can fuse with a mobile

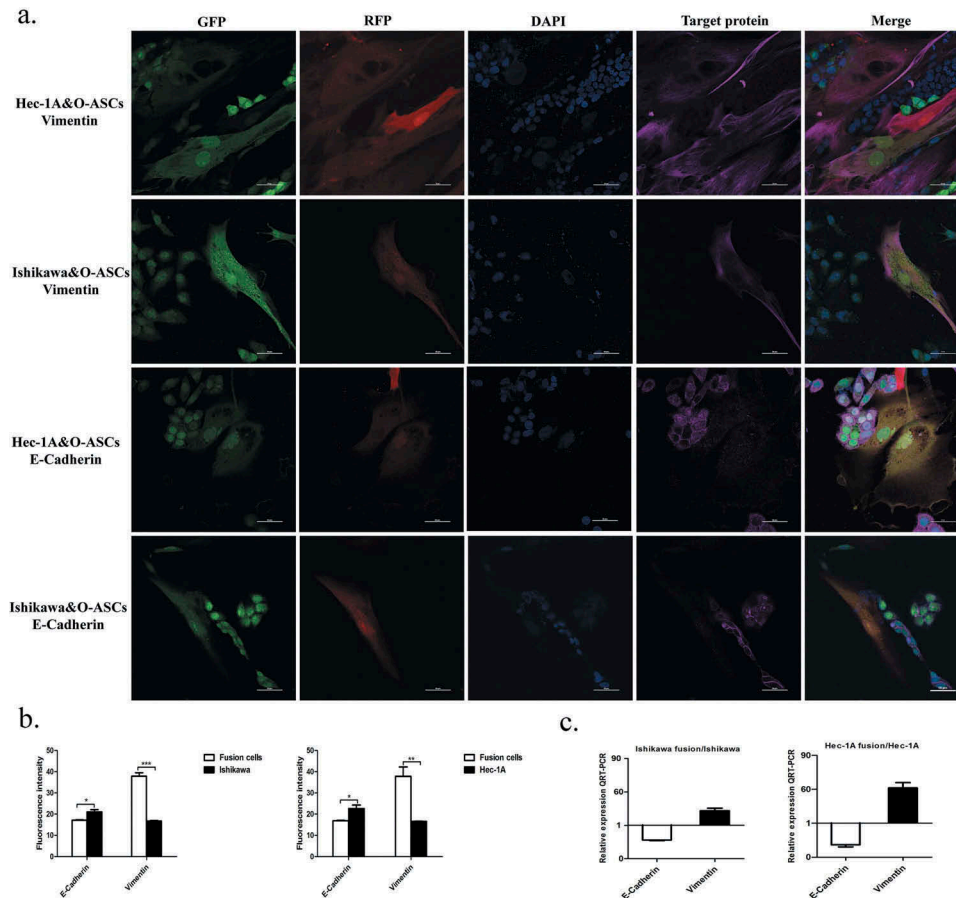


Figure 5. Fusion with O-ASCs induces EMT in endometrial cancer cells. (a). Immunofluorescent staining for E-cadherin and Vimentin in the hybrid cells and their parental cells. (b). Semi-quantitative expression analysis of E-cadherin and Vimentin was performed by a High-Throughput Imaging Analysis. (c). The expression of EMT-related genes was determined by real-time RT-PCR. The experiments were repeated three times. The statistical results are presented as Means \pm SD. * $P < 0.05$, *** $P < 0.001$.

cell type and then travel to another site in the body to establish cancer. This is the classic “cancer cell fusion” theory [38], which was the first to regard cell fusion as a possible mechanism of tumor metastasis. Pawelek et al. fused healthy macrophages with weakly metastatic melanoma cells and found that most of the experimental hybrids were highly metastatic and lethal when implanted into mice [31]. They showed this in an animal model and then substantiated their findings in reports showing that cancer cell fusion occurs in humans. They described two patients who suffered from renal-cell carcinomas that possessed a donor-patient hybrid genome after bone marrow transplantation [27,28,34]. Thus, cell fusion events may be regarded as a hidden force or enemy in cancer [21].

A large number of studies have explored the formation of hybrids between myeloid and tumor cells.

Pawelek JM proposed that fusion between tumor and bone marrow-derived cells is a unifying explanation for metastasis [31]. Xu et al. found that tumorigenic hybrids between bone marrow-derived MSCs and lung cancer cell lines lost their epithelial morphology, assumed a fibroblast-like appearance and exhibited increased malignancy and prometastatic traits [33]. Another report suggested that the formation of MSC-breast cancer cell hybrids was a potential mechanism underlying the generation of invasive/metastatic breast cancer cells [29]. In summary, these studies indicate that hybrids between myeloid cells and tumor cells contribute to tumor progression. Currently, very few reports have described cell fusion between ASCs and cancer cells. ASCs have features that are similar to those of BM-MSCs, which can also be recruited to the tumor stroma, where they promote the acceleration of migration and metastasis in cancer cells, including endometrial cancer [20,39–41].

However, the mechanisms underlying these effects might involve their ability to affect the expression of paracrine cytokines.

In our study, we found that O-ASCs spontaneously fused with Ishikawa and Hec-1A EC cells. The resulting hybrid cells lost their round and polygonal morphology, assumed an elongated and fibroblast-like appearance, exhibited mesenchymal phenotypes and properties of ASCs in addition to increased metastatic capacity. Under an Opera high-throughput spinning-disk confocal microscopy system, we found that the fused cells were hyperactive compared to their parental cells. Their migratory speed was far faster than the speed observed in O-ASCs and EC cells. Further experiments indicated that the fused cells expressed higher levels of markers and regulatory genes and proteins associated with EMT, including an obvious decrease in E-cadherin expression and increase in vimentin expression, and this likely contributed to their enhanced motility in migration assays. These data indicate that cell fusion events may induce EMT in the resulting hybrids, and EMT is an essential step during the process of cancer cell dissemination and metastasis. This phenomenon was also observed in MSC and gastric cancer cell hybrids and lung cancer and breast cancer cell hybrids and contributed to cancer progression [30,33].

As previously reported, cell fusion promotes phenotypic and genotypic diversity in tumors [42]. When accompanied by cell fusion, centrosome amplification may lead to multipolar division and chromosomal instability, resulting in a heterogeneous pool of aneuploid cells [25]. However, centrosome doubling after cell fusion does not always lead to chromosomal instability because the extra centrioles can be discarded, coalesced or orphaned, allowing tumor cells to maintain the ability to undergo bipolar division with two functional centrosomes [43]. In addition, the ability of hybrids to sustain a relatively stable genomic composition allows tumor cells to acquire and stably maintain additional malignant properties [24,44]. In this study, we found that the multiple nuclei that formed as a result of cell fusion possessed the ability to spontaneously fuse into a single nucleus immediately before cell division. The fused cells could undergo either bipolar or multipolar division, and this might help to explain why their chromosomes were

aneuploid. Through multipolar division the hybrids formed by O-ASCs and EC cells were capable of dividing to achieve proliferation which also increased heterogeneity of cancer cells.

After the O-ASCs and EC cells fused, they underwent EMT, which provided them with a new phenotype that enhanced their migratory capacity. In addition, by undergoing multipolar division, the fused cells obtained a new genotype, and this may have helped them to increase heterogeneity during cancer progression. These data represent just the very beginning of our study, and our aim is to identify more characteristics of fused cells, including those related to their stemness, drug resistance and metastasis, to fully explore the true significance of fusion.

Material and methods

Cell culture

The Ishikawa line of endometrial adenocarcinoma cells [estrogen receptor (ER)- and progesterone receptor (PR)-positive] was obtained from laboratory stocks and cultured in 5% CO₂ at 37°C in DMEM/F12 (Cat. C11330500BT, Gibco, USA) supplemented with 10% fetal bovine serum (FBS, Cat.10099–141, Gibco, USA). Another endometrial adenocarcinoma cell line, Hec-1A [estrogen receptor (ER)- and progesterone receptor (PR)-negative], was purchased from ATCC (Manassas, VA, USA) in 2015 (Lot NO. 58087755) and cultured in 5% CO₂ at 37°C in H-DMEM (Cat. C12430500BT, Gibco, USA) supplemented with 10% FBS (Cat.10099–141, Gibco, USA). Cell passages 3 to 10 after thawing were used for the experiments. Cultured cells were routinely tested for viability with trypan blue exclusion and maintained high viability (>95%). And the minute fraction of dead cells was predominantly removed by washing before trypsinization. DNA fluorescence staining method were used to exclude mycoplasma infection.

Isolation of omental adipose tissue-derived stromal cells

Grossly normal-appearing human omentum was obtained during staging procedures with approval from the institutional review board of Peking

University People's Hospital. O-ASC1 tissues were isolated from a patient (BMI = 23.05) with moderate differentiated endometrioid adenocarcinoma. O-ASC2 tissues were isolated from a patient (BMI = 24.08) with adenosquamous carcinoma of the endometrium. O-ASC3 tissues were isolated from a patient (BMI = 30.05) with well-differentiated endometrioid adenocarcinoma. The omentum samples obtained from these three patients appeared grossly normal without metastasis. The tissues were subjected to mechanical disruption followed by digestion with 0.075% type I collagenase (Cat.17100017, Invitrogen, USA) for 30 minutes at 37°C. The digested adipose tissue was centrifuged at 1,000 rpm for 10 minutes. The supernatant containing the adipocytes was removed, and the cell pellet was resuspended in α -minimum essential medium (α -MEM, Cat. SH30265.01B, HyClone, USA). The resuspended cells were filtered through a 100-mm cell strainer (Becton Dickinson). Red blood cells were lysed in 5 ml of RBC Lysis Buffer (Cat. #786-649, G-Bioscience, USA) and incubated in a 37°C water bath for 10 minutes. The remaining mononuclear cells were resuspended and seeded in α -MEM supplemented with 10% FBS and 1% penicillin-streptomycin at 37°C in a humidified atmosphere containing 5% CO₂. O-ASCs between passages 3 and 6 were used in the experiments.

O-ASC characterization

After isolation, the cells were expanded in vitro and then characterized by flow cytometry to evaluate cell surface marker expression. All O-ASCs were characterized at passages 3–6 using antibodies against the following mesenchymal stem cell markers: CD34-APC, CD44-FITC, CD45-PE-cy5, CD29-APC, CD73-PE, CD90-PE, CD11b-PE-cy5, HLA-DR-PE and CD105-PE (Becton Dickinson, Franklin Lakes, NJ, USA). Their catalog numbers and corresponding isotype controls (Becton Dickinson, Franklin Lakes, NJ, USA) were showed in supplemental Table 1.

Studies aimed at exploring cell differentiation, including the adipogenic, osteoblastic and chondrogenic potentials of the cells, were conducted as previously reported [19].

Generation of GFP-expressing cells

Ishikawa and Hec-1A EC cells were labeled with GFP using a GFP control lentiviral vector (Genechem, China). The titers of the viral stocks were determined by calculating the percentage of GFP-positive cells that were transduced in serially diluted viral suspensions. To induce transduction, Ishikawa and Hec-1A cells were seeded at moderate density overnight. Two h before transduction, the medium was changed, and the transductions were then carried out for 12 h in the presence of 5 mg/ml polybrene (Cat.107689, Sigma, USA). The GFP-positive cells were sorted and further expanded for subsequent experiments.

Generation of RFP-expressing cells

O-ASCs were labeled with RFP using an RFP control lentiviral vector (Genechem, China). The titers of the viral stocks were determined by calculating the percentage of RFP-positive cells that were transduced in serially diluted viral suspensions. To induce transduction, O-ASCs were seeded at moderate density overnight. Two h before transduction, the medium was changed, and the transductions were then carried out for 12 h in the presence of 5 mg/ml polybrene (Cat.107689, Sigma, USA). The RFP-positive cells were sorted and further expanded for subsequent experiments.

Cell fusion

Cell fusion was captured by directly co-culturing RFP-labeled-O-ASCs (O-ASCs/RFP) and GFP-labeled-EC cells (Ishikawa/GFP&Hec-1A/GFP) in 96-well plates (PerkinElmer, Inc.). O-ASCs/RFP (1000 cells/well) and Ishikawa/GFP (500 cells/well) cells were co-cultured in ASC growth medium in 96-well plates. After the cells had been co-cultured for 48 h, Hoechst 33242 (Sigma, USA) was applied for 30 minutes to stain the nuclei. Then, the plates were put in a PerkinElmer Opera High Content System (PerkinElmer, USA) and incubated in a humidified atmosphere of 37°C that contained 5% CO₂ to promote cell survival. Bright-field and fluorescence microscopy photographs of 11 high-power fields in each well were automatically taken by the system

every 1 h for a continuous 24 h. The same treatment was applied to the Hec-1A cells. Images of the cell fusions resulting from RFP-labeled-O-ASCs and GFP-labeled-Hec-1A/Ishikawa cells were also captured and analyzed. At least three independent sets of experiments were performed.

Chromosome preparation

RFP-labeled-O-ASCs (2×10^5) and GFP-labeled-Hec-1A/Ishikawa cells (1×10^5) were co-cultured in ASC growth medium in T75 culture flasks for 3 days. Then, the fused cells were sorted by a flow cytometer (FACS Calibur, BD Biosciences, USA). The double-positive fusion cells were collected in ASC growth medium. The sorted fused cells were collected and cultured in T25 culture flasks. At the same time, O-ASCs/RFP, Ishikawa/GFP and Hec-1A/GFP cells were cultured in T25 flasks in ASC growth medium. When all the cells had grown to 80%-90% confluence, we used them to prepare chromosomes, as previously reported. After the slides were prepared and submitted to solid staining, we observed the cells under a light microscope at 10X and 100X magnification and randomly selected 10 chromosome karyotypes for statistical analysis.

Cell fusion efficiency

RFP-labeled-O-ASCs (O-ASCs/RFP) and GFP-labeled-EC cells (Ishikawa/GFP&Hec-1A/GFP) were co-cultured directly in 96-well plates (PerkinElmer, Inc.). The proportions of O-ASCs/RFP (1000 cells/well) and GFP-labeled-EC cells were 1:1,1:2,1:3,1:4,1:5,1:6,1:7,1:8,1:9 and 1:10 respectively. After the cells had been co-cultured for 24h, Hoechst 33242 (Cat. B2261, Sigma, USA) was applied for 30 minutes to stain the nuclei. Then, Bright-field and fluorescence microscopy photographs of 11 high-power fields in each well were automatically taken by the PerkinElmer Opera High Content System (PerkinElmer, USA) every day for 8 days. The system can capture fusion cells and the parental cells for their different fluorescence, count cell numbers and calculate cell fusion efficiency. At least three independent sets of experiments were performed.

Proliferation and migration of fused cells

The proliferation and migration of the fused cells were captured following the direct co-culture of O-ASCs/

RFP cells and EC/GFP cells (Ishikawa/GFP&Hec-1A/GFP) in 96-well plates (PerkinElmer, Inc.). The experimental methods were the same as those used to observe cell fusion. Cells that were both red and green double-positive were recognized as fused cells and distinguished from single-positive cells (O-ASCs/RFP and EC cells/GFP) under a fluorescence microscope. Their proliferation and divisions were dynamically observed at each time point. Meanwhile, the speed of migration of both the double-positive fused cells and the single-positive unfused cells (O-ASCs and EC cells) was determined at each time point and calculated by the microscopy equipment. To intuitively obtain the details related to hybrid cell division and migration, the sequences were captured at each time point and compiled into a video. The mean migratory speeds over 24 h were also analyzed. At least three independent sets of experiments were performed.

Immunofluorescence

RFP-labeled-O-ASCs (2.5×10^4) and GFP-labeled-Hec-1A/Ishikawa cells (2.5×10^4) were co-cultured in ASC growth medium in confocal dishes for 48 h. After we confirmed under a fluorescence microscope that fused cells had formed, the cells were washed twice with cold PBS, fixed with 4% paraformaldehyde for 15 min, permeabilized with 0.1% Triton X-100 for 5 min, blocked with 5% BSA, incubated with the indicated primary antibodies including anti-E-Cadherin (Cat.#3195, CST, USA) and anti-Vimentin (Cat.#5741, CST, USA) at 4°C overnight and then incubated with an Alexa Fluor 647-conjugated anti-rabbit secondary antibody (Cat. A281281, Invitrogen, USA). The cells were then stained with DAPI (Cat. D1306, Invitrogen, USA) to visualize the nuclei, and images were acquired with a Nikon eclipse Ti-S microscope (Nikon, Tokyo, Japan).

Real-time RT-PCR

RFP-labeled-O-ASCs (2×10^5) and GFP-labeled-Hec-1A/Ishikawa cells (1×10^5) were co-cultured in ASC growth medium in T75 culture flasks for 3 days. Then, the fused cells and EC cells were sorted by a flow cytometer (FACS Calibur, BD Biosciences, USA). The double-positive fusion cells were fusion cells

and GFP-positive cells were EC cells. Total RNA was extracted using Trizol reagent (Cat.15596026, Invitrogen, USA) according to the manufacturer's instructions and equal amount of RNA was used for real-time PCR analyzes. The cDNAs were synthesized by using a reverse transcription kit (Cat. KR107-02, TIANGEN, China). was used as the internal control. The sequences of specific primers are listed as follows: E-Cadherin, Forward, TTTGACGCCGAGAGCTAC AC; Reverse, AATTC ACTCTGCC CAGGACG. Vimentin, Forward, AAATGGCTCGTCACCTTC GT; Reverse, CAGCTTCCTGTAGGTGGCAA. GAPDH, Forward, GCACCGTCAAGGCTGAGA AC, Reverse, TGGTGAAGACGCCAGTGGA. At least three independent sets of experiments were performed.

High-throughput imaging analysis

O-ASCs/RFP (500 cells/well) and EC/GFP (Ishikawa or Hec-1a, 500 cells/well) cells were co-cultured in ASC growth medium in 96-well plates (PerkinElmer, Inc.). After the cells were co-cultured for 48 h, IF staining was performed (see Immunofluorescence). The cells were then imaged in a single optimal focal plane (11 fields/well with a 10x water immersion objective) on an Opera high-throughput spinning-disk confocal microscopy system (Perkin Elmer). Sequential images were acquired with 647, 488 and 568 nm excitation lasers. Cells that were double-positive for red and green were recognized as fused cells, while cells positive for only green were considered EC/GFP cells (controls). The results of immunofluorescence (IF) were analyzed at the single-cell level with a customized algorithm [45] using DAPI-based nuclear segmentation to quantify the total nuclear intensity of all indicated targets. All recognized cells were analyzed, and quantifications are shown as the average of each population of cells and were determined with a 647 nm excitation laser in each well. In addition, the intensity of the fluorescence in each well was quantified with Image J software. At least three independent sets of experiments were performed.

Statistical analysis

All experiments were performed at least 3 times, and all data are expressed as the means±SEM.

Statistical significance was determined by T-tests using Prism5 software (GraphPad, La Jolla, CA, USA). A P value of less than 0.05 was considered to be statistically significant.

Acknowledgments

The authors thanks Yu Wang and Meng Lai for technical help in High-Throughput imaging Analysis.

Author contributions

Mingxia Li and Xiaoping Li, Acquisition of data, Analysis and interpretation of data, Drafting or revising the article; Lijun Zhao, Jingyi Zhou, Yuan Cheng and Bo Xu, Acquisition of data, Contributed to construction; Jianliu Wang, Conception and design, Drafting or revising the article. Lihui Wei, Conception and design.

Disclosure statement

No potential conflict of interest was reported by the authors.

Funding

This study was supported by National Key R&D Program of China under Grant 2016YFC1303100.

ORCID

Lihui Wei  <http://orcid.org/0000-0002-2478-8790>

References

- [1] Chen W, Sun K, Zheng R, et al. Cancer incidence and mortality in China, 2014. *Chin J Cancer Res.* 2018;30:1–12. PMID: 29545714.
- [2] Zheng R, Zeng H, Zhang S, et al. Estimates of cancer incidence and mortality in China, 2013. *Chin J Cancer.* 2017;36:66. PMID: 28818111.
- [3] Friedenreich C, Cust A, Lahmann PH, et al. An anthropometric factors and risk of endometrial cancer: the European prospective investigation into cancer and nutrition. *Cancer Causes Contr.* 2007;18:399–413. PMID: 17297555.
- [4] Prizment AE, Flood A, Anderson KE, et al. Survival of women with colon cancer in relation to precancer anthropometric characteristics: the Iowa women's Health Study. *Cancer Epidemiol Biomarkers Prev.* 2010;19:2229–2237. PMID: 20826830.

- [5] Balentine CJ, Enriquez J, Fisher W, et al. Intra-abdominal fat predicts survival in pancreatic cancer. *J Gastrointest Surg.* 2010;14:1832–1837. PMID: 20725799.
- [6] Murphy TK, Calle EE, Rodriguez C, et al. Body mass index and colon cancer mortality in a large prospective study. *Am J Epidemiol.* 2000;152:847–854. PMID: 11085396.
- [7] Kaaks R, Van Noord PA, Den Tonkelaar I, et al. Breast-cancer incidence in relation to height, weight and body-fat distribution in the Dutch “DOM” cohort. *Int J Cancer.* 1998;76:647–651. PMID: 9610720.
- [8] Männistö S, Pietinen P, Pyy M, et al. Body-size indicators and risk of breast cancer according to menopause and estrogen-receptor status. *Int J Cancer.* 1996;68:8–13. PMID: 8895532.
- [9] Xu WH, Matthews CE, Xiang YB, et al. Effect of adiposity and fat distribution on endometrial cancer risk in Shanghai women. *Am J Epidemiol.* 2005;161:939–947. PMID: 15870158.
- [10] Arsenault BJ, Lachance D, Lemieux I, et al. Visceral adipose tissue accumulation, cardiorespiratory fitness, and features of the metabolic syndrome. *Arch Intern Med.* 2007;167:1518–1525. PMID: 17646606.
- [11] Zhang C, Rexrode KM, van Dam RM, et al. Abdominal obesity and the risk of all-cause, cardiovascular, and cancer mortality: sixteen years of follow-up in US women. *Circulation.* 2008;117:1658–1667. PMID: 18362231.
- [12] Kidd S, Spaeth E, Watson K, et al. Origins of the tumor microenvironment: quantitative assessment of adipose-derived and bone marrow-derived stroma. *PLOS ONE.* 2012;7:e30563. PMID: 22363446.
- [13] Karp JM, Leng Teo GS. Mesenchymal stem cell homing: the devil is in the details. *Cell Stem Cell.* 2009;4:206–216. PMID: 19265660.
- [14] Zhang Y, Daquinag AC, Amaya-Manzanares F, et al. Stromal progenitor cells from endogenous adipose tissue contribute to pericytes and adipocytes that populate the tumor microenvironment. *Cancer Res.* 2012;72:5198–5208. PMID: 23071132.
- [15] Freese KE, Kokai L, Edwards RP, et al. Adipose-derived stem cells and their role in human cancer development, growth, progression, and metastasis: a systematic review. *Cancer Res.* 2015;75:1161–1168. PMID: 25736688.
- [16] Zhang Y, Daquinag A, Traktuev DO, et al. White adipose tissue cells are recruited by experimental tumors and promote cancer progression in mouse models. *Cancer Res.* 2009;69:5259–5266. PMID: 19491274.
- [17] Rowan BG, Gimble JM, Sheng M, et al. Human adipose tissue-derived stromal/stem cells promote migration and early metastasis of triple negative breast cancer xenografts. *PLOS ONE.* 2014;9:e89595. PMID: 24586900.
- [18] Strong AL, Strong TA, Rhodes LV, et al. Obesity associated alterations in the biology of adipose stem cells mediate enhanced tumorigenesis by estrogen dependent pathways. *Breast Cancer Res.* 2013;15:R102. PMID: 24176089.
- [19] Nowicka A, Marini FC, Solley TN, et al. Human omental-derived adipose stem cells increase ovarian cancer proliferation, migration, and chemoresistance. *PLOS ONE.* 2013;8:e81859. PMID: 24312594.
- [20] Klopp AH, Zhang Y, Solley T, et al. Omental adipose tissue-derived stromal cells promote vascularization and growth of endometrial tumors. *Clin Cancer Res.* 2012;18:771–782. PMID: 22167410.
- [21] Duelli D, Lazebnik Y. Cell fusion: a hidden enemy? *Cancer Cell.* 2003;3:445–448. PMID:12781362.
- [22] Ogle BM, Cascalho M, Platt JL. Biological implications of cell fusion. *Nat Rev Mol Cell Biol.* 2005;6:567–575. PMID: 15957005.
- [23] Chakraborty AK, Sodi S, Rachkovsky M, et al. A spontaneous murine melanoma lung metastasis comprised of host x tumor hybrids. *Cancer Res.* 2000;60:2512–2519. PMID: 10811133.
- [24] Lu X, Kang Y. Cell fusion as a hidden force in tumor progression. *Cancer Res.* 2009;69:8536–8539. PMID: 19887616.
- [25] Lu X, Kang Y. Efficient acquisition of dual metastasis organotropism to bone and lung through stable spontaneous fusion between MDA-MB-231 variants. *Proc Natl Acad Sci U S A.* 2009;106:9385–9390. PMID: 19458257.
- [26] Pawelek JM. Tumour cell hybridization and metastasis revisited. *Melanoma Res.* 2000;10:507–514. PMID: 11198471.
- [27] Vignery A. Macrophage fusion: the making of osteoclasts and giant cells. *J Exp Med.* 2005;202:337–340. PMID: 16061722.
- [28] Busund LT, Killie MK, Bartnes K, et al. Spontaneously formed tumorigenic hybrids of Meth A sarcoma cells and macrophages in vivo. *Int J Cancer.* 2003;106:153–159. PMID: 12800188.
- [29] Ding J, Jin W, Chen C, et al. Tumor associated macrophage x cancer cell hybrids may acquire cancer stem cell properties in breast cancer. *PLOS ONE.* 2012;7:e41942. PMID: 22848668.
- [30] Rappa G, Mercapide J, Lorico A. Spontaneous formation of tumorigenic hybrids between breast cancer and multipotent stromal cells is a source of tumor heterogeneity. *Am J Pathol.* 2012;180:2504–2515. PMID: 22542847.
- [31] Pawelek JM, Chakraborty AK. Fusion of tumour cells with bone marrow-derived cells: a unifying explanation for metastasis. *Nat Rev Cancer.* 2008;8:377–386. PMID: 18385683.
- [32] Xue J, Zhu Y, Sun Z, et al. Tumorigenic hybrids between mesenchymal stem cells and gastric cancer cells enhanced cancer proliferation, migration and stemness. *BMC Cancer.* 2015;15:793. PMID: 26498753.
- [33] Xu MH, Gao X, Luo D, et al. EMT and acquisition of stem cell-like properties are involved in spontaneous formation of tumorigenic hybrids between lung cancer

- and bone marrow-derived mesenchymal stem cells. *PLOS One*. 2014;9:e87893. PMID: 24516569.
- [34] Pawelek JM. Tumour-cell fusion as a source of myeloid traits in cancer. *Lancet Oncol*. 2005;6:988–993. PMID: 16321767.
- [35] Dominici M, Le Blanc K, Mueller I, et al. Minimal criteria for defining multipotent mesenchymal stromal cells. The International Society for Cellular Therapy position statement. *Cytotherapy*. 2006;8:315–317. PMID: 16923606.
- [36] Daquinag AC, Zhang Y, Kolonin MG. Vascular targeting of adipose tissue as an anti-obesity approach. *Trends Pharmacol Sci*. 2011;32:300–307. PMID: 21349592.
- [37] Rachkovsky M, Sodi S, Chakraborty A, et al. Melanoma x macrophage hybrids with enhanced metastatic potential. *Clin Exp Metastasis*. 1998;16:299–312. PMID: 9626809.
- [38] Pawelek JM. Cancer-cell fusion with migratory bone-marrow-derived cells as an explanation for metastasis: new therapeutic paradigms. *Future Oncol*. 2008;4:449–452. PMID: 18684055.
- [39] Gomes CM. The dual role of mesenchymal stem cells in tumor progression. *Stem Cell Res Ther*. 2013;4:42. PMID: 23680129.
- [40] Zhu W, Huang L, Li Y, et al. Exosomes derived from human bone marrow mesenchymal stem cells promote tumor growth in vivo. *Cancer Lett*. 2012;315:28–37. PMID: 22055459.
- [41] Luo F, Liu T, Wang J, et al. Bone marrow mesenchymal stem cells participate in prostate carcinogenesis and promote growth of prostate cancer by cell fusion in vivo. *Oncotarget*. 2016;24(7):30924–30934. PMID: 27129157.
- [42] Warner TF. Cell hybridization: an explanation for the phenotypic diversity of certain tumours. *Med Hypotheses*. 1975;1:51–57. PMID: 1105094.
- [43] Brinkley BR. Managing the centrosome numbers game: from chaos to stability in cancer cell division. *Trends Cell Biol*. 2001;11:18–21. PMID:11146294.
- [44] Quintyne NJ, Reing JE, Hoffelder DR, et al. Spindle multipolarity is Prevented by centrosomal clustering. *Science*. 2005;307:127–129. PMID: 15637283.
- [45] Kubben N, Brimacombe KR, Donegan M, et al. A high-content imaging-based screening pipeline for the systematic identification of anti-progeroid compounds. *Methods*. 2016;96:46–58. PMID: 26341717.